Available online at www.sciencedirect.com
ScienceDirect
Journal of Environmental Sciences 2010, 22(8) 1273–1280
JOURNAL OF ENVIRONMENTAL SCIENCES
ISSN 1001-0742
CN 11-2629/X
www.jesc.ac.cn

Application of activated carbon derived from scrap tires for adsorption of Rhodamine B

Li Li[1], Shuangxi Liu[1,*], Tan Zhu[2]

1. Institute of New Catalytic Materials Science, College of Chemistry, Nankai University, Tianjin 300071, China. E-mail: lillyfeng@mail.nankai.edu.cn
2. College of Environmental Science and Engineering, Nankai University, Tianjin 300071, China

Received 09 October 2009; revised 05 January 2010; accepted 08 January 2010

Abstract

Activated carbon derived from solid hazardous waste scrap tires was evaluated as a potential adsorbent for cationic dye removal. The adsorption process with respect to operating parameters was investigated to evaluate the adsorption characteristics of the activated pyrolytic tire char (APTC) for Rhodamine B (RhB). Systematic research including equilibrium, kinetics and thermodynamic studies was performed. The results showed that APTC was a potential adsorbent for RhB with a higher adsorption capacity than most adsorbents. Solution pH and temperature exert significant influence while ionic strength showed little effect on the adsorption process. The adsorption equilibrium data obey Langmuir isotherm and the kinetic data were well described by the pseudo second-order kinetic model. The adsorption process followed intra-particle diffusion model with more than one process affecting the adsorption process. Thermodynamic study confirmed that the adsorption was a physisorption process with spontaneous, endothermic and random characteristics.

Key words: activated pyrolytic tire char; Rhodamine B; adsorption isotherm; thermodynamics
DOI: 10.1016/S1001-0742(09)60250-3

Introduction

Hazards associated with scrap tires can cause both health and environmental problems (Jang et al., 1998). The accumulation of scrap tires results in large spaces occupied and a wastage of a valuable energy resource. The huge amount and high stability of scrap tires have made their disposal a serious environmental problem. Although pyrolysis is considered as an effective and environmental friendly disposal method, a proper utilization for the residues generated is still a problem to be solved (de Marco Rodriguez et al., 2001). Pyrolytic tire char accounts for 30%–40% of the original tire mass, and its utilization significantly determines the profitability of the tire pyrolysis process at industrial scale (Kaminsky and Mennerich, 2001; Ko et al., 2004; Piskorz et al., 1999). However, the complexity and the presence of contaminants such as ash, sulfur containing byproducts and oily condensates, have restricted the direct application of the pyrolytic tire char.

One potential application for the pyrolytic tire char is to produce activated carbon (Cunliffe and Williams, 1998; Ko et al., 2004; Li et al., 2005; Mui et al., 2004; Teng et al., 2000; Zabaniotou and Stavropoulos, 2003). These tire-derived activated carbons have been applied for the adsorption of effluent pollutants such as phenols (Helleur et al., 2001; Nakagawa et al., 2004; San Miguel et al., 2002; Tanthapanichakoon et al., 2005), heavy metal ions (Hamadi et al., 2001), pesticides (Hamadi et al., 2004), and dyes (Garcia et al., 2007; Nakagawa et al., 2004; San Miguel et al., 2002; Tanthapanichakoon et al., 2005). Their application in gaseous phase has also been studied and was found to be feasible for the removal of acetone, trichlorethane, mercury chloride, and mercury (Lehmann et al., 1998; Manchón-Vizuete et al., 2005; Seneviratne et al., 2007; Skodras et al., 2007).

However, in previous works, the pyrolytic tire char studied in pollution control is limited to laboratory or pilot scale (Garcia et al., 2007; Hamadi et al., 2001, 2004; Helleur et al., 2001; Lehmann et al., 1998; Manchón-Vizuete et al., 2005; Nakagawa et al., 2004; San Miguel et al., 2002; Seneviratne et al., 2007; Skodras et al., 2007; Tanthapanichakoon et al., 2005), and no research work has been done on pyrolytic tire char in industrial scale.

Highly colored wastewater containing hazardous dyes is another serious environmental problem. The high organic concentration, toxicity, complex composition and poor degradability of dye-containing wastewater have impeded the development of efficient purification and treatment methods. At present, the studies of dye removal by pyrolytic tire char (Garcia et al., 2007; Nakagawa et al., 2004; San Miguel et al., 2002; Tanthapanichakoon et al., 2005) were mainly limited in Methylene Blue. Moreover, only adsorption capacity was examined, whereas adsorption kinetics,

* Corresponding author. E-mail: sxliu@nankai.edu.cn

thermodynamics and effect of operating parameters on the adsorption process have not been studied. These properties are vital in supplying the basic information required for the design and operation of adsorption process. In addition, the difference in the nature of adsorbates could make the adsorption process different. Therefore, it is necessary to study the adsorption phenomena of other class of dyes. Rhodamine B (RhB) is a highly water soluble, basic red dye of the xanthene class. It is a typical cationic dye that has been widely used as a colorant in textiles and food stuffs. It is also a well-known water tracer fluorescent and biological stains.

It would be a promising and effective way to treat the wastewater by the activated carbon derived from scrap tires. The present study aims to assess the applicability of activated carbon derived from the industrial-scale pyrolytic tire char for the adsorptive removal of RhB from aqueous solution and to investigate the kinetics and mechanism of the adsorption process. The system variables studied include initial dye concentration, adsorbent dosage, temperature, initial solution pH and ionic strength.

1 Materials and methods

1.1 Materials

Pyrolytic tire char was obtained from an industrial pyrolysis plant with annual processing capacity of 10,000 tons of scrap tires in Shanghai Greenman ECO Science and Technology Co., Ltd., China. Activated pyrolytic tire char (APTC) was prepared according to our previous patent (Liu et al., 2008). Briefly, pyrolytic tire char was treated first by toluene to remove the rudimental pyrolysis oil and subsequently by dilute acid to remove inorganic ashes. After that, steam activation was performed at 800°C for 3 hr. The structure characteristics of APTC were investigated by N_2 adsorption-desorption on Tristar 3000 (Micromeritics, America). The value of the pH required to give zero net surface charge, point of zero charge (pH_{pzc}) of APTC was determined by the pH drift test (Rivera-Utrilla et al., 2001).

RhB ($C_{28}H_{31}N_2O_3Cl$; maximum absorption wavelength 556 nm), analytical grade, was purchased from Yingdaxigui Chemical Ind. Ltd. (Tianjin, China). Its chemical structure is shown in Fig. 1. Absorbance measurements were carried out on a 2550 UV-Visible spectrophotometer (Schimadzu, Japan).

1.2 Adsorption studies

Batch experiments were performed to investigate the adsorption process of RhB by the APTC. For each experimental run, 100 mL of RhB solution of known concentration, initial pH, ionic strength and the amount of the APTC were taken in a 250-mL stoppered conical flask. This mixture was agitated in a temperature-controlled shaking water bath at a constant speed of 200 r/min and certain temperatures.

For adsorption equilibrium studies, RhB solutions of different concentrations (20–150 mg/L) were contacted with a certain amount of APTC under certain conditions for 12 hr insuring the equilibrium was achieved. The residual RhB concentration was then measured and the amount of RhB adsorbed onto APTC was calculated

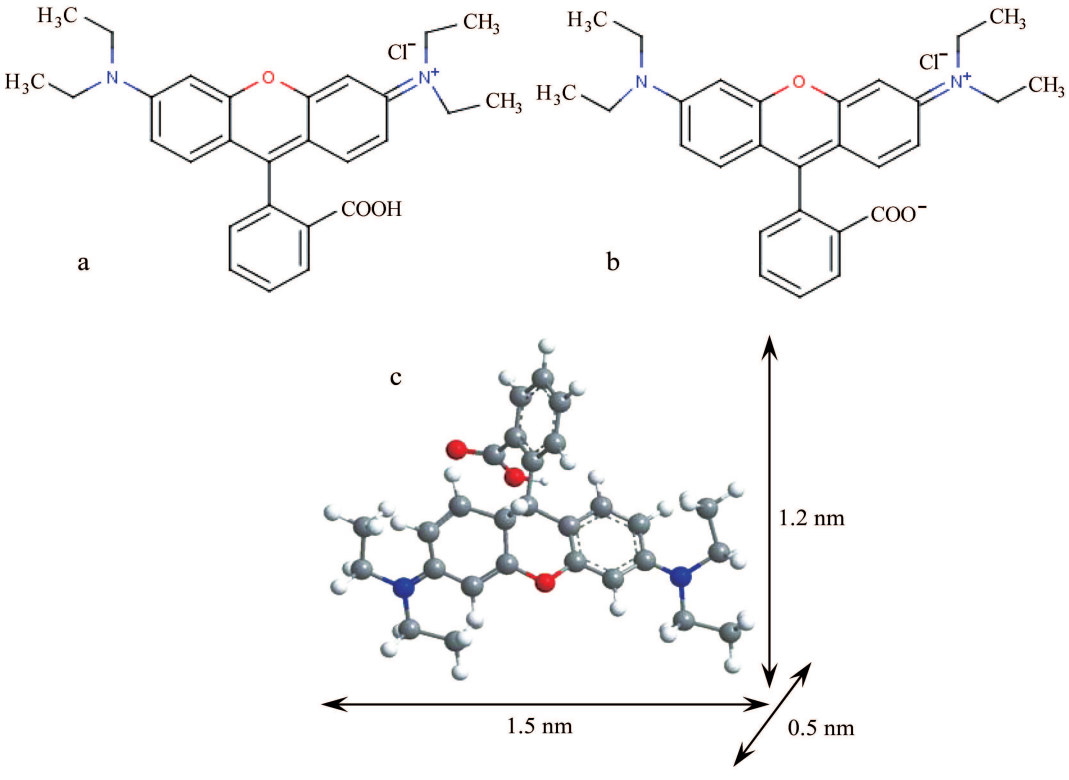

Fig. 1 Chemical structure of RhB. (a) cationic form; (b) zwitterionic form; (c) three dimensional structure.

from mass balance. Effects of contact time, adsorbent dosage, initial RhB concentration, initial solution pH, ionic strength and temperature) on RhB adsorption by APTC were investigated.

Adsorption kinetics was determined by analyzing adsorptive uptake of RhB from aqueous solution at different time intervals. The amount of RhB adsorbed at time t, q_t (mg/g), was calculated using mass balance equation.

2 Results and discussion

2.1 Characterization of APTC

The structure parameters evaluated from N_2 adsorption-desorption analysis and physicochemical characteristics of APTC are listed in Table 1, and compared with other forms of activated carbon from literature. It can be seen that APTC has similar BET surface area with other forms of activated carbon. The porosity of APTC is well developed with higher percentage of mesopore structure and larger average pore size, which are advantageous for dye adsorption. As indicated in Table 1, the pH_{pzc} of APTC is about 6.7, thus, the surface charge of APTC is positive when solution pH is lower than 6.7, and vice versa.

Table 1 Physicochemical characteristics of activated pyrolytic tire char (APTC) and other activated carbon from literature

Parameter	Adsorbent		
	APTC	Sago waste activated carbon[a]	BPH activated carbon[b]
BET surface area (m^2/g)	720	625	523
Total pore volume (cm^3/g)	1.05	0.67	0.39
Mesopore volume (cm^3/g)	0.92	–	0.30
Average pore diameter D_{BJH} (nm)	8.7	–	3.0
Point of zero charge, pH_{pzc}	6.7	5.7	3.9

[a] Kadirvelu et al., 2005; [b] Gad and El-Sayed, 2009.

2.2 Adsorption capacity

Herein, the effect of operation parameters on the adsorption capacity of APTC for RhB was investigated. In addition, the observed adsorption equilibrium data were fitted by the Langmuir and Freundlich isotherms.

2.2.1 Effect of operation parameters on adsorption capacity

The effect of temperature on the adsorption capacity of APTC is shown in Fig. 2. It can be seen that the adsorption capacity is almost independent of temperature but significantly positively dependent on initial RhB concentration at lower initial concentrations (20–50 mg/L). However, when initial RhB concentration is higher than 50 mg/L, an increase of temperature enhances APTC's adsorption capacity, while the increase of RhB concentration has little impact on APTC's adsorption capacity. The main reason is that at the lower concentrations, the APTC could adsorb almost all of RhB. According to the mass balance equation, the APTC adsorption capacity positively increases with initial RhB concentration, while temperature has no significant influence under this condition. As for RhB concentrations higher than 50 mg/L, the APTC is saturated. Therefore, the increase of initial concentration has no influence on adsorption capacity while the temperature could affect the adsorption capacity. The enhancement of adsorption capacity of APTC at higher temperatures can be attributed to the following reason. The thermal motion of RhB molecules becomes more frequent at higher temperatures, which is favorable for more RhB molecules to be adsorbed by the same amount of APTC.

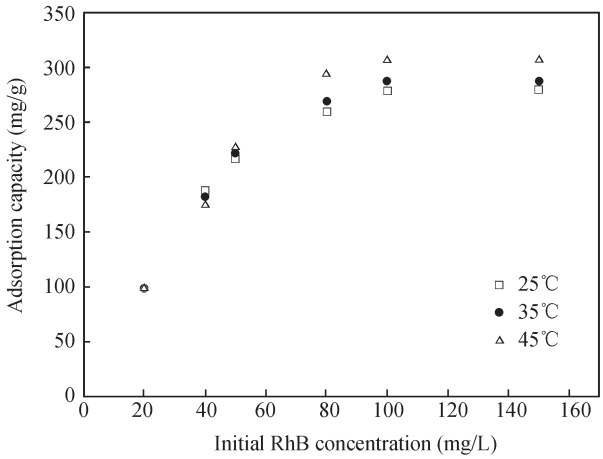

Fig. 2 Effect of temperature on the adsorption capacity of APTC. Conditions: natural pH; NaCl concentration 0; adsorbent dosage 0.2 g/L.

The solution pH plays an important role in the whole adsorption process and particularly on the adsorption capacity. The effect of initial solution pH on APTC adsorption capacity for RhB is presented in Fig. 3. The maximum removal (around 100%) for RhB was found at pH 4.0. The removal decreased to about 80% at highly acidic condition (pH 3.0) and reached minimum (about 75%) at pH 7.0. However, when the pH of the solution was further increased (> 7.0), the uptake of RhB increased to over 97%. Therefore, both acidic and basic solutions are suitable for RhB removal.

RhB is an aromatic amino acid with amphoteric characteristics due to the presence of both the amino group

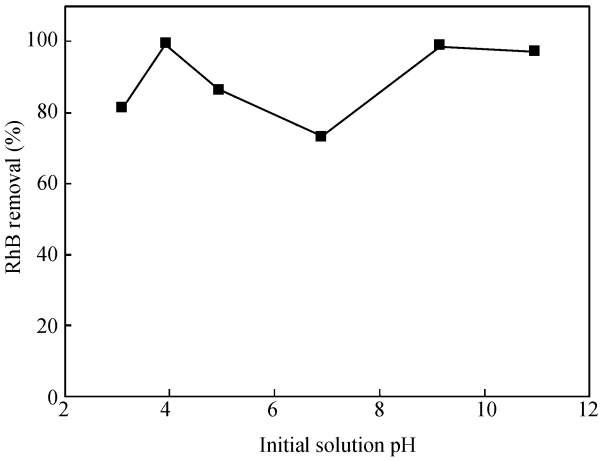

Fig. 3 Effect of initial solution pH on the adsorption capacity of APTC. Conditions: temperature 25°C; initial RhB concentration 50 mg/L; adsorbent dosage 0.2 g/L; NaCl concentration 0.

($-NHR_2$) and the carboxyl group (–COOH). Thus, the charge state of RhB is dependent on solution pH. The pKa value for the aromatic carboxyl group presented on the RhB molecule is about 4.0. When the solution pH is lower than 4.0, the RhB ion takes on a positive charge on one of the nitrogens while the carboxyl group is unionized (Fig. 1a). The electrostatic repulsion between cationic RhB and positively charged APTC leads to the decreased percentage of adsorption when pH decreased from 4.0 to 3.0. When solution pH increased above 4.0, the carboxyl group gets ionized and the zwitterions form of RhB (Fig. 1b) is formed (Deshpande and Kumar, 2002). The zwitterion form of RhB in water may increase dimerization of RhB, which makes the molecule too large to enter most of the pore structure of APTC. The inaccessibility to the pore structure of APTC, which is smaller than the dimer's effective size, resulted in a decrease in RhB removal. The greater aggregation of the zwitterionic form is due to the electrostatic attraction between the carboxyl and xanthane groups of the monomer. When the pH is higher than 7.0, excessive OH^- compete with COO^- in binding with $-N^+$ and the aggregation of RhB decreases. Therefore, an increase in the adsorption of RhB on the APTC can be observed at pH > 7.0. The variation of RhB removal with solution pH is similar to that reported previously (Arivoli et al., 2008; Guo et al., 2005), but is different from other adsorbents (Selvam et al., 2008; Sureshkumar and Namasivayam, 2008).

NaCl is commonly used in textile dyeing processes as an additive to promote the adsorption capacity of the textile fibers. Furthermore, industrial effluents are always contaminated by various additives such as inorganic salts. Thus, the effect of ionic strength on the adsorption process was studied at three NaCl concentrations and the result is shown in Fig. 4. The influence of ionic strength on the adsorption rate would be discussed on the Section 2.3.2.

The adsorption capacity of APTC for RhB was slightly affected by the presence of NaCl (Fig. 4). There is a carboxyl group (–COOH) in the RhB molecule, which imparts a negative charge to the chromophore. A positive charge is also contributed by the amino group. When the ionic strength increased, the electrical double layer surrounding the APTC surface was compressed, resulting in a decrease in RhB adsorption onto APTC. On the other hand, NaCl could screen the electrostatic interaction of the opposite-charged groups in the zwitterionic RhB molecules, and the adsorbed amount will increase with the increase of NaCl concentration. As a result of the above two opposite influences, adsorption capacity of APTC for RhB is little affected by ionic strength.

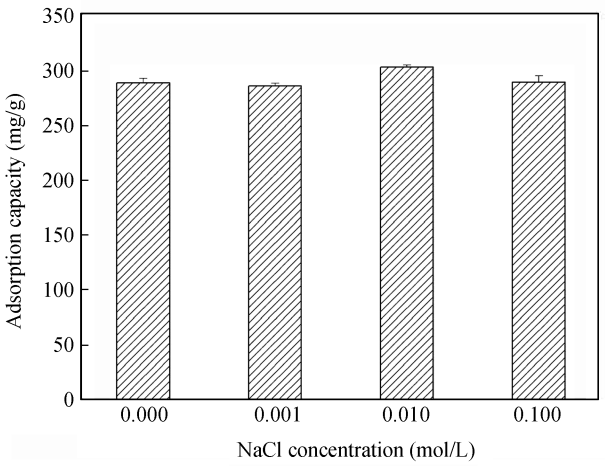

Fig. 4 Effect of ionic strength on the adsorption capacity of APTC. Conditions: initial RhB concentration 100 mg/L; natural pH; temperature 25°C; adsorbent dosage 0.2 g/L.

2.2.2 Adsorption isotherm

The equilibrium adsorption isotherm is essential in describing the interactive behavior between adsorbate and adsorbent, and is important in the design of adsorption systems. Several adsorption isotherm equations are available and the two important isotherms, i.e., the Langmuir isotherm and Freundlich isotherm, are selected in this study.

The linear form of Langmuir isotherm is given by the following Eq. (1):

$$\frac{C_e}{q_e} = \frac{1}{bQ_0} + \frac{C_e}{Q_0} \tag{1}$$

where, C_e and q_e are the equilibrium liquid-phase and solid-phase of concentration, respectively; Q_0 (mg/g) is the monolayer capacity of the adsorbent; and b (L/mg) is the Langmuir adsorption constant, which is related to the adsorption energy.

The Freundlich isotherm is described by the following Eq. (2):

$$\log q_e = \log K_F + \frac{1}{n}\log C_e \tag{2}$$

where, K_F (L/g) and n are the Freundlich constants of the system, indicators of adsorption capacity and adsorption intensity, respectively.

The values of Langmuir and Freundlich parameters at different temperatures are shown in Table 2. It can be seen that the correlation coefficient (R^2) for Langmuir isotherm model is higher than 0.99, and q_{max} calculated from the model is close to the experimental data. This indicates that the adsorption feature of APTC could be well described by the Langmuir isotherm. However, the Freundlich isotherm does not fit well with the equlibrium data. In addition, it is observed that adsorption capacity is positively correlated with temperature. The maximum adsorption capacity of APTC for RhB is 307.2 mg/g, which is significantly higher than those reported for most of the other adsorbents (Table 3).

2.3 Adsorption kinetics

In order to effectively apply APTC for a particular pollutant removal from aqueous solution, it is important to study the kinetics and mechanism of the adsorption process. Moreover, information of adsorption kinetics is required for selecting the optimum operating conditions for the full-scale batch process. Herein, the kinetics of adsorption removal of RhB by APTC is studied, and influence of operating parameters on the adsorption rate is also evaluated.

Table 2 Langmuir and Freundlich isotherms model constants and respective coefficients for RhB adsorption onto APTC

Temperature (°C)	Experimental	Langmuir model			Freundlich model		
	q_{max} (mg/g)	Q_0 (mg/g)	b (L/mg)	R^2	K_F (L/g)	n	R^2
25	280.1	277.8	1.31	0.9998	134.1	4.59	0.9264
35	288.4	285.7	2.19	0.9993	112.7	3.37	0.9139
45	307.2	312.5	3.89	0.9995	134.2	4.73	0.9411

Table 3 Comparison of APTC adsorption capacity for RhB with other adsorbents

Adsorbent	Q_0 (mg/g)	Reference
Surfactant-modified coconut coir pitch	14.9	Sureshkumar and Namasivayam, 2008
Sago waste derived activated carbon	16.1	Kadirvelu et al., 2005
Sodium montmorillonite	42.2	Selvam et al., 2008
Jute stick powder	87.7	Panda et al., 2009
Carbonaceous adsorbent	91.1	Bhatnagar and Jain, 2005
BPH activated carbon	263.9	Gad and El-Sayed, 2009
Rice husk-based porous carbons (RHCs)	383.4	Guo et al., 2005
APTC	307.2	This work

2.3.1 Kinetics study

The pseudo first- and second-order models were employed to perform the kinetics study. The linear form of the pseudo first-order rate expression is given as Eq. (3):

$$\ln(q_e - q_t) = \ln q_e - k_1 t \tag{3}$$

where, k_1 (min^{-1}) is the rate constant of the pseudo first-order adsorption. The pseudo second-order kinetic model is expressed by the following Eq. (4):

$$\frac{t}{q_t} = \frac{1}{k_2 q_e^2} + \frac{t}{q_e} \tag{4}$$

where, k_2 (g/(mg·min)) is the rate constant of the pseudo second-order model. The initial rate h (mg/(g·min)) can be determined using Eq. (5):

$$h = k_2 q_e^2 \tag{5}$$

The validity of the two kinetic models can be checked by their linearized plots. The correlation coefficient (R^2) was used to compare the applicability of different kinetic models in fitting the experimental data. Table 4 shows the corresponding parameters of the two kinetic models under different conditions. Based on R^2, the pseudo second-order kinetic model is well fitted to the experimental data. Furthermore, the q_e calculated from the pseudo second-order kinetic model is close to the experimental data.

2.3.2 Effect of experimental parameters on adsorption rate

The effect of contact time on adsorbed amount of RhB at three adsorbent dosages is shown in Fig. 5. It is obvious that there is a rapid uptake of RhB within the first 60 min. Then, the adsorption rate slows down gradually and no further adsorption is observed beyond 300 min. With the increase of adsorbent dosage, the time needed to reach equilibrium is reduced. This is due to the increase of efficient adsorption sites at higher dosages. On the contrary, the initial rate h is reduced from 68.4 to 17.9 mg/(g·min) when adsorbent dosage is increased from 0.1 to 0.5 g/L (Table 4). This can be attributed to the increased viscosity of the solution, which hinders the diffusion of RhB ions to the surface of APTC.

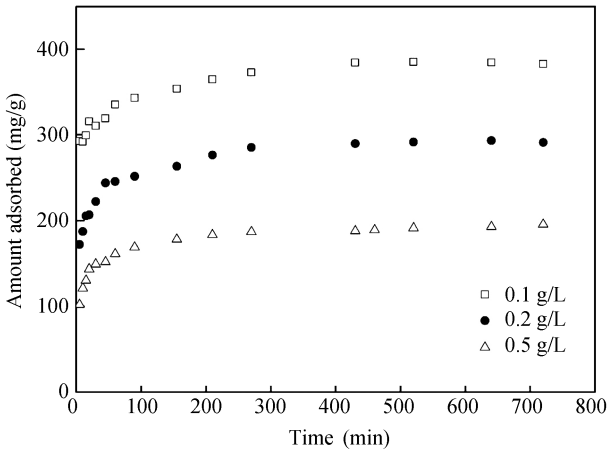

Fig. 5 Effect of contact time and adsorbent dosage on adsorption kinetics. Conditions: temperature 25°C; natural pH; initial RhB concentration 100 mg/L.

As shown in Fig. 6, the removal rate of RhB is dependent on the initial RhB concentration. The rate of adsorption decreased with time until it gradually approached a plateau

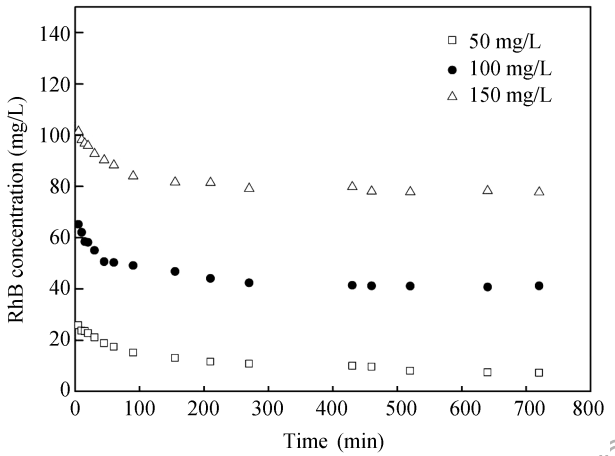

Fig. 6 Effect of contact time and initial RhB concentration on adsorption kinetics. Conditions: temperature 25°C; natural pH; NaCl concentration 0; adsorbent dosage 0.2 g/L.

Table 4 Parameters of kinetic models of RhB adsorption onto APTC

Adsorption condition	$q_{e,exp}$ (mg/g)	Pseudo first-order model			Pseudo second-order model				Intra-particle diffusion model					
		k_1 (min^{-1})	$q_{e,cal}$ (mg/g)	R^2	k_2 ($\times 10^3$ g/(mg·min))	$q_{e,cal}$ (mg/g)	R^2	h	k_{i1} (mg/(g·$min^{1/2}$))	C	R^2	k_{i2} (mg/(g·$min^{1/2}$))	C	R^2
Adsorbent dosage[a] (g/L)														
0.1	384.4	0.0125	128.1	0.9253	0.463	384.6	0.9980	68.4	7.46	273.4	0.9314	1.81	335.4	0.6288
0.2	280.1	0.0079	92.9	0.9802	0.339	284.1	0.9997	27.3	11.4	155.3	0.9245	2.22	239.1	0.8229
0.5	195.6	0.0050	55.4	0.9273	0.467	196.1	0.9996	17.9	8.49	95.1	0.8924	1.32	161.1	0.9209
Initial concentration[b] (mg/L)														
50	211.2	0.0060	83.6	0.9178	0.301	212.7	0.9987	13.6	7.30	103.8	0.9920	2.16	154.9	0.9668
100	280.1	0.0063	79.9	0.9206	0.339	284.1	0.9997	27.3	11.4	155.3	0.9245	2.22	239.1	0.8229
150	280.8	0.1030	119.9	0.9203	0.360	287.1	0.9998	29.6	11.7	219.5	0.9957	1.64	319.7	0.8574
Temperature[c] (°C)														
25	280.1	0.0063	79.9	0.9206	0.339	284.1	0.9997	27.3	8.93	166.9	0.8777	1.73	249.9	0.7665
35	288.4	0.0167	170.6	0.7807	0.406	290.8	0.9989	34.3	15.5	114.6	0.9600	3.06	215.4	0.8727
45	307.2	0.0285	241.5	0.5871	0.484	310.8	0.9982	46.7	14.9	127.1	0.9737	4.35	207.6	0.9671
pH[d]														
3.04	289.2	0.0179	164.7	0.7508	0.422	294.1	0.9989	36.5	14.8	133.9	0.9666	3.79	216.1	0.9325
7.03	256.4	0.0158	138.6	0.7759	0.404	260.3	0.9992	27.5	14.2	122.2	0.9902	2.82	210.9	0.9559
10.0	268.6	0.0165	168.9	0.6878	0.399	270.3	0.9983	29.1	12.1	129.0	0.9576	3.83	192.7	0.9826
Ionic strength[e] (mol/L)														
0.001	277.5	0.0082	139.7	0.4731	0.296	277.8	0.9994	22.8	8.96	146.9	0.8869	1.93	225.3	0.9215
0.010	293.8	0.0073	119.9	0.5180	0.314	294.1	0.9995	27.1	8.42	169.2	0.8896	1.82	245.2	0.8513
0.100	280.9	0.0101	178.4	0.4708	0.218	285.7	0.9989	17.7	7.72	148.9	0.8098	2.62	213.7	0.9058

[a] Conditions: temperature 25°C; natural pH; initial RhB concentration 100 mg/L; NaCl concentration 0.
[b] Conditions: temperature 25°C; natural pH; adsorbent dosage 0.2 g/L; NaCl concentration 0.
[c] Conditions: natural pH; adsorbent dosage 0.2 g/L; initial RhB concentration 100 mg/L; NaCl concentration 0.
[d] Conditions: temperature 35°C; adsorbent dosage 0.2 g/L; initial RhB concentration 100 mg/L; NaCl concentration 0.
[e] Conditions: temperature 25°C; natural pH; adsorbent dosage 0.2 g/L; initial RhB concentration 100 mg/L.

due to the continuous decrease in the concentration driving force. In addition, it can be seen from Table 4 that the initial rate of adsorption h was greater at higher initial RhB concentrations, as the resistance to the RhB uptake decreased with the increase of mass transfer driving force.

The effect of temperature on adsorption was investigated under natural solution pH. As shown in Table 4, the adsorption rate constant and initial rate increase with temperature. Owing to the decrease in the viscosity of the solution at higher temperature, the diffusion of RhB across the external boundary layer and in the internal pores of the APTC particle is enhanced. Therefore, the observed overall adsorption rate improves with the increase of temperature.

As presented in Table 4, among the studied three initial solution pH, the initial adsorption rate h reaches maximum at pH 3.04 and minimum at pH 7.03. The variation in the adsorption rate of RhB with pH can be elucidated by considering the dissociation form of RhB. When solution pH is lower than 4.00, RhB molecules mainly exist as small cationic ions, which diffuse faster and could access to most of the surface of APTC. However, deprotonation of RhB takes place with increasing solution pH, which leads to the formation of larger zwitterions. The larger zwitterions have lower diffusivities and thus a decrease in the adsorption rate is observed. When solution pH is further increased above 7.00, the excessive OH^- compete with COO^- in binding with $-N^+$, leading to a decrease in the aggregation of RhB. Therefore, an increase in the adsorption rate of RhB ions on the APTC is observed.

The effect of ionic strength on the adsorption rate of RhB is also displayed in Table 4. It can be observed that the presence of inorganic salt exerted a slight influence on the adsorption rate of RhB. The possible reason is that the presence of the positive charge from the amino group and the negative charge from the carboxyl group, made NaCl has little effect on the electrical character of the RhB molecule. Therefore, the adsorption rate is little affected by ionic strength.

2.4 Adsorption mechanism

The pseudo second-order kinetic model includes all the steps of adsorption including external film diffusion, internal particle diffusion, and surface adsorption. The experimentally observed adsorption rate is also the overall rate of the whole process. Therefore, it is necessary to predict the rate-limiting step of the adsorption process.

Two diffusion steps are necessary for the adsorption of the adsorbate onto the adsorbent in aqueous solution, i.e., mass transfer from water to the adsorbent surface across the boundary layer and diffusion in the porous particle. Generally, film diffusion is often the rate-limiting step in a continuous flow system, while for a batch reactor intra-particle diffusion is more likely the rate-limiting step (McKay, 1983). The possibility of intra-particle diffusion as rate-limiting step was tested by intra-particle diffusion model, which is defined as Eq. (6):

$$q_t = k_{ip} t^{1/2} + C \tag{6}$$

where, k_{ip} (mg/(g·$min^{1/2}$)) is the intra-particle diffusion rate constant. The value of C is helpful in determining the boundary thickness: a larger C corresponding to a greater boundary layer diffusion effect (Kannan and Sundaram, 2001).

By the plots of q_t versus $t^{1/2}$ of various initial RhB concentrations, multilinearities can be observed in Fig. 7, indicating that intra-particle diffusion plays a significant role but is not the only rate-controlling step. The first and

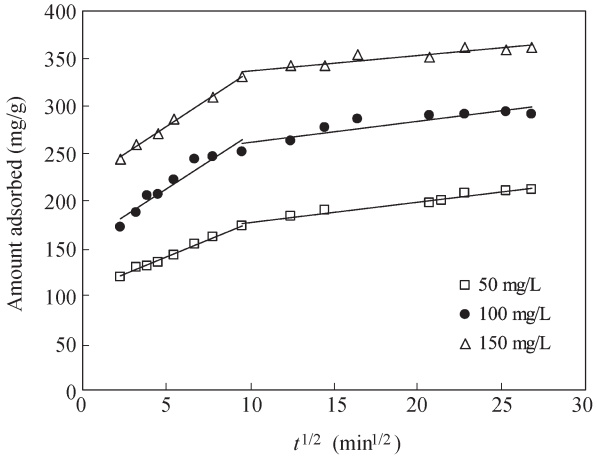

Fig. 7 Intra-particle diffusion plots under different initial RhB concentrations. Conditions: temperature 25°C; natural pH; NaCl concentration 0; adsorbent dosage 0.2 g/L.

sharper portion is attributed to the boundary layer diffusion of RhB molecules. The second portion corresponds to the gradual adsorption stage, where intra-particle diffusion was rate-limiting step. The slope of the second linear portion of the plot was defined as the intra-particle diffusion parameter k_{i2}. Table 4 shows the corresponding model fitting parameters under different conditions. The observed values of k_{i2} are lower than k_{i1}, indicating that intra-particle diffusion controls the adsorption rate. However, external mass transfer resistance cannot be neglected although this resistance is only significant for the initial period of time. The variations of k_{i2} with adsorption conditions are also consistent with the observations in Section 2.3.2.

2.5 Adsorption thermodynamics

In order to fully understand the nature of the adsorption process studied, thermodynamic studies were performed. Thermodynamic parameters such as change in free energy (ΔG^0), enthalpy (ΔH^0) and entropy (ΔS^0) were calculated using the following equations:

$$\Delta G^0 = -RT\ln b \tag{7}$$

$$\ln b = \frac{\Delta S^0}{R} - \frac{\Delta H^0}{RT} \tag{8}$$

where, b (L/mol) is Langmuir constants at different temperatures, R (8.314 J/(K·mol)) is the universal gas constant.

Thermodynamic parameters at various temperatures are presented in Table 5. The negative values of ΔG^0 indicate that the adsorption of RhB onto APTC is spontaneous and thermodynamically favorable. Moreover, when the temperature increases from 25 to 45°C, ΔG^0 changes from –15.96 to –19.91 kJ/mol, suggesting that adsorption is more spontaneous at higher temperature. The positive value of ΔH^0 (42.82 kJ/mol) indicates that the process is endothermic in nature, which is supported by the increase in the adsorption capacity of APTC for RhB with increasing temperature. Moreover, the positive value of ΔS^0 (197.1 J/(K·mol)) suggests that the randomness increased at the solid-liquid interface during the adsorption of RhB in aqueous solution on the APTC.

Table 5 Thermodynamic parameters at various temperatures

Temperature (°C)	$-\Delta G^0$ (kJ/mol)	ΔH^0 (kJ/mol)	ΔS^0 (J/(K·mol))	E_a (kJ/mol)
25	15.96	42.82	197.1	13.99
35	17.81			
45	19.91			

As mentioned in Section 2.3.1, the pseudo second-order kinetic model fits well to the adsorption process of RhB by APTC. Accordingly, the rate constants (k_2) of the pseudo second-order model are adopted to calculate the activation energy of the adsorption process using the Arrhenius equation (Doğan and Alkan, 2003):

$$\ln k_2 = \ln A - \frac{E_a}{RT} \tag{9}$$

where, k_2, A, E_a, R and T are the rate constant of the pseudo second-order model, Arrhenius factor, activation energy, gas constant and temperature, respectively. The activation energy could be determined from the slope of the plot of $\ln k_2$ versus $1/T$ (figure not shown). The activation energy (E_a) in this study is 13.99 kJ/mol, further confirming that the adsorption process is mainly physical. Therefore, ΔG^0, ΔH^0 and E_a all suggest that the adsorption of RhB onto APTC is mainly a physisorption process.

3 Conclusions

The present study shows that APTC derived from solid hazardous scrap tires can be used as a potential adsorbent for the removal of RhB with a higher adsorption capacity (307.2 mg/g) than most adsorbents reported in literature. Adsorption equilibrium is practically achieved within 300 min. Both acidic and basic solutions are suitable for the adsorption process, and temperature exerts strong positive influence on the adsorption process. However, ionic strength shows only slight effect on the adsorption process. High initial RhB concentration and low APTC dosage are favorable for adsorption process. Langmuir isotherm can be successfully applied to predict the adsorption capacities of the adsorbent, and the adsorption kinetics follows the pseudo second-order rate expression. The removal rate of RhB is dependent on both external mass transfer and intra-particle diffusion. Changes in free energy of adsorption (ΔG^0), enthalpy (ΔH^0) and entropy (ΔS^0), as well as the activation energy (E_a) confirm that the adsorption of RhB onto APTC is mainly a physisorption process with spontaneous, endothermic, and random characteristics.

Acknowledgments

This work was supported by the National Key Technologies R & D Program of China (No. 2006BAC02A12), the Key Technologies R & D Program of Tianjin, China (No. 07ZCGYSH02000), and the Natural Science Foundation of Tianjin, China (No. 08JCZDJC21400).

References

Arivoli S, Sundaravadivelu M, Elango K P, 2008. Removal of basic and acidic dyes from aqueous solution by adsorption on a low cost activated carbon: Kinetic and thermodynamic study. *Indian Journal of Chemical Technology*, 15(2): 130–139.

Bhatnagar A, Jain A K, 2005. A comparative adsorption study with different industrial wastes as adsorbents for the removal of cationic dyes from water. *Journal of Colloid and Interface Science*, 281(1): 49–55.

Cunliffe A M, Williams P T, 1998. Properties of chars and activated carbons derived from the pyrolysis of used tyres. *Environmental Technology*, 19(12): 1177–1190.

de Marco Rodriguez I, Laresgoiti M F, Cabrero M A, Torres A, Chomón M J, Caballero B, 2001. Pyrolysis of scrap tyres. *Fuel Processing Technology*, 72(1): 9–22.

Deshpande A V, Kumar U, 2002. Effect of method of preparation on photophysical properties of Rh-B impregnated sol-gel hosts. *Journal of Non-Crystalline Solids*, 306(2): 149–159.

Doğan M, Alkan M, 2003. Adsorption kinetics of methyl violet onto perlite. *Chemosphere*, 50(4): 517–528.

Gad H M H, El-Sayed A A, 2009. Activated carbon from agricultural by-products for the removal of Rhodamine-B from aqueous solution. *Journal of Hazardous Materials*, 168(2-3): 1070–1081.

Garcia I T S, Nunes M R, Carreo N L V, Wallaw W M, Fajardo H V, Probst L F D, 2007. Preparation and characterization of activated carbons from thread of tire waste. *Polímeros*, 17: 329–333.

Guo Y P, Zhao J Z, Zhang H, Yang S F, Qi J R, Wang Z C et al., 2005. Use of rice husk-based porous carbon for adsorption of Rhodamine B from aqueous solutions. *Dyes and Pigments*, 66(2): 123–128.

Hamadi N K, Chen X D, Farid M M, Lu M G Q, 2001. Adsorption kinetics for the removal of chromium(VI) from aqueous solution by adsorbents derived from used tyres and sawdust. *Chemical Engineering Journal*, 84(2): 95–105.

Hamadi N K, Swaminathan S, Chen X D, 2004. Adsorption of paraquat dichloride from aqueous solution by activated carbon derived from used tires. *Journal of Hazardous Materials*, 112(1-2): 133–141.

Helleur R, Popovic N, Ikura M, Stanciulescu M, Liu D, 2001. Characterization and potential applications of pyrolytic char from ablative pyrolysis of used tires. *Journal of Analytical and Applied Pyrolysis*, 58-59: 813–824.

Jang J W, Yoo T S, Oh J H, Iwasaki I, 1998. Discarded tire recycling practices in the United States, Japan and Korea. *Resources, Conservation and Recycling*, 22(1-2): 1–14.

Kadirvelu K, Karthika C, Vennilamani N, Pattabhi S, 2005. Activated carbon from industrial solid waste as an adsorbent for the removal of Rhodamine-B from aqueous solution: Kinetic and equilibrium studies. *Chemosphere*, 60(8): 1009–1017.

Kaminsky W, Mennerich C, 2001. Pyrolysis of synthetic tire rubber in a fluidised-bed reactor to yield 1,3-butadiene, styrene and carbon black. *Journal of Analytical and Applied Pyrolysis*, 58: 803–811.

Kannan N, Sundaram M M, 2001. Kinetics and mechanism of removal of methylene blue by adsorption on various carbons – a comparative study. *Dyes and Pigments*, 51(1): 25–40.

Ko D C K, Mui E L K, Lau K S T, McKay G, 2004. Production of activated carbons from waste tire – process design and economical analysis. *Waste Management*, 24(9): 875–888.

Lehmann C M B, Rostam-Abadi M, Rood M J, Sun J, 1998. Reprocessing and reuse of waste tire rubber to solve air-quality related problems. *Energy & Fuels*, 12(6): 1095–1099.

Li S Q, Yao Q, Wen S E, Chi Y, Yan J H, 2005. Properties of pyrolytic chars and activated carbons derived from pilot-scale pyrolysis of used tires. *Journal of the Air & Waste Management Association*, 55(9): 1315–1326.

Liu S X, Zhang C, Liang X Q, Zhang X, Zhu T, 2008. Patent No: CN101164876-A.

Manchón-Vizuete E, Macías-García A, Nadal Gisbert A, Fernández-González C, Gómez-Serrano V, 2005. Adsorption of mercury by carbonaceous adsorbents prepared from rubber of tyre wastes. *Journal of Hazardous Materials*, 119(1-3): 231–238.

McKay G, 1983. The adsorption of dyestuffs from aqueous solution using activated carbon: Analytical solution for batch adsorption based on external mass transfer and pore diffusion. *Chemical Engineering Journal*, 27(3): 187–196.

Mui E L K, Ko D C K, McKay G, 2004. Production of active carbons from waste tyres – A review. *Carbon*, 42(14): 2789–2805.

Nakagawa K, Namba A, Mukai S R, Tamon H, Ariyadejwanich P, Tanthapanichakoon W, 2004. Adsorption of phenol and reactive dye from aqueous solution on activated carbons derived from solid wastes. *Water Research*, 38(7): 1791–1798.

Panda G C, Das S K, Guha A K, 2009. Jute stick powder as a potential biomass for the removal of Congo Red and Rhodamine B from their aqueous solution. *Journal of Hazardous Materials*, 164(1): 374–379.

Piskorz J, Majerski P, Radlein D, Wik T, Scott D S, 1999. Recovery of carbon black from scrap rubber. *Energy & Fuels*, 13(3): 544–551.

Rivera-Utrilla J, Bautista-Toledo I, Ferro-Garcia M A, Moreno-Castilla C, 2001. Activated carbon surface modifications by adsorption of bacteria and their effect on aqueous lead adsorption. *Journal of Chemical Technology and Biotechnology*, 76(12): 1209–1215.

San Miguel G, Fowler G D, Sollars C J, 2002. Adsorption of organic compounds from solution by activated carbons produced from waste tyre rubber. *Separation Science and Technology*, 37(3): 663–676.

Selvam P P, Preethi S, Basakaralingam P, Thinakaran N, Sivasamy A, Sivanesan S, 2008. Removal of Rhodamine B from aqueous solution by adsorption onto sodium montmorillonite. *Journal of Hazardous Materials*, 155(1-2): 39–44.

Seneviratne H R, Charpenteau C, George A, Millan M, Dugwell D R, Kandiyoti R, 2007. Ranking low cost sorbents for mercury capture from simulated flue gases. *Energy & Fuels*, 21(6): 3249–3258.

Skodras G, Diamantopouiou I, Zabaniotou A, Stavropoulos G, Sakellaropoulos G P, 2007. Enhanced mercury adsorption in activated carbons from biomass materials and waste tires. *Fuel Processing Technology*, 88(8): 749–758.

Sureshkumar M V, Namasivayam C, 2008. Adsorption behavior of direct Red 12B and Rhodamine B from water onto surfactant-modified coconut coir pith. *Colloids and Surfaces A: Physicochemical and Engineering Aspects*, 317(1-3): 277–283.

Tanthapanichakoon W, Ariyadejwanich P, Japthong P, Nakagawa K, Mukai S R, Tamon H, 2005. Adsorption-desorption characteristics of phenol and reactive dyes from aqueous solution on mesoporous activated carbon prepared from waste tires. *Water Research*, 39(7): 1347–1353.

Teng H S, Lin Y C, Hsu L Y, 2000. Production of activated carbons from pyrolysis of waste tires impregnated with potassium hydroxide. *Journal of the Air & Waste Management Association*, 50(11): 1940–1946.

Zabaniotou A A, Stavropoulos G, 2003. Pyrolysis of used automobile tires and residual char utilization. *Journal of Analytical and Applied Pyrolysis*, 70(2): 711–722.